

Asymmetric profiles observed in the recombination of Bi^{79+} : A benchmark for relativistic theories involving interference

Nobuyuki Nakamura,¹ Anthony P. Kavanagh,² Hirofumi Watanabe,³ Hiroyuki A. Sakaue,⁴ Yueming Li,⁵ Daiji Kato,⁴ Fred J. Currell,² Xiao-Min Tong,^{6,7} Tsutomu Watanabe,¹ and Shunsuke Ohtani¹

¹*Institute for Laser Science, The University of Electro-Communications, Chofu, Tokyo 182-8585, Japan*

²*Queen's University Belfast, Belfast BT7 1NN, United Kingdom*

³*Chubu University, Kasugai-shi, Aichi 487-8501, Japan*

⁴*National Institute for Fusion Science, Toki, Gifu 509-5292, Japan*

⁵*Institute of Applied Physics and Computational Mathematics, P.O. Box 8009, Beijing 100088, China*

⁶*Doctoral Program in Materials Science, Graduate School of Pure and Applied Sciences, University of Tsukuba, Tsukuba, Ibaraki 305-8573, Japan*

⁷*Center for Computational Sciences, University of Tsukuba, Tsukuba, Ibaraki 305-8577, Japan*

(Received 19 March 2009; published 31 July 2009)

Asymmetric profiles have been observed in the recombination cross section of Be-like Bi obtained by measuring the electron energy dependence of the ion abundance ratio in an electron-beam ion trap. In contrast to the previous x-ray measurements, the present measurement gives the integrated recombination cross section with higher statistical quality, which provides a benchmark to test the relativistic theory involving the interference between the resonant and continuum states. The comparison with our theoretical study shows that the Breit interaction plays an important role in this case.

DOI: [10.1103/PhysRevA.80.014503](https://doi.org/10.1103/PhysRevA.80.014503)

PACS number(s): 31.15.am, 34.80.Lx, 34.10.+x, 52.20.Fs

Interference between different paths is a general phenomenon in quantum physics. A typical example is that a resonant state embedded into continuum states results in an asymmetric line profile in the photoabsorption spectra [1]. The observed spectra have been well explained by the Fano line profile [2] expressed as

$$f(E) = \frac{(q + \varepsilon)^2}{(q^2 + 1)(1 + \varepsilon^2)}, \quad \varepsilon = \frac{E - E_r}{\Gamma/2}. \quad (1)$$

Here E_r is the resonant energy and Γ is the natural width of the resonant state, and q is the shape parameter, which is proportional to the ratio between the transition matrix element to the resonant state and the one to the continuum state. A significant asymmetric profile should be observed when the q value is on the order of one. If the q value is very large, the line profile becomes symmetric. The asymmetric structures associated with photoabsorption or its inverse process radiative recombination (RR) have been studied extensively during the past several decades especially for light atoms. For highly charged heavy ions, an asymmetric line profile was first observed with the high-energy electron-beam ion trap (super EBIT) at Lawrence Livermore National Laboratory [3] by measuring emitted x rays due to recombination. When the incident electron is at the correct energy (a resonant energy), it is captured by the HCl nonradiatively and excites another electron in the HCl. The autoionization state thus formed will decay to stable states by emitting one or more x rays, which enhances the observed x-ray intensity. This is a typical dielectric recombination (DR) process. An asymmetric profile of the x-ray emission was observed due to *KLL* DR resonance of He- to B-like U ($Z=92$) ions. *KLL* means that the incident electron is captured into the *L* shell accompanying the excitation of another electron from *K* shell to *L* shell. In their measurements, the contributions from dif-

ferent charge states could not be resolved because they were mixed in the EBIT. The interference was also observed for Hg ($Z=80$) ions with the Heidelberg EBIT [4] and for Bi ($Z=83$) ions with the Tokyo EBIT [5]. Although the contributions from the different charge states were not clearly resolved, these measurements were used to determine the shape parameters q for each resonant state by only including a narrow part of the RR line chosen to include predominantly the contribution from only one or two charge states. The observed asymmetric profile can be explained as a Fano line profile due to a bound state, formed by the DR process, and embedded into the continuum states.

We have studied the DR resonant feature by measuring the electron energy dependence of the ion abundance at equilibrium [6]. The abundance was obtained by measuring the intensity of ions extracted from the EBIT. Since the total (extraction, transport, and detection) efficiency of the ion measurement is about 10%, the present method is more efficient than the previous x-ray measurements, where only a fraction (typically less than 0.1%) of the radiation emitted into 4π solid angle is collected so that many hours would be required to get enough statistics. For example, around 100 h were needed for the Hg measurement with the Heidelberg EBIT. Apart from improving the statistical quality of the experiment, we have also performed a theoretical study by the Green's function method and our theoretical simulations successfully reproduced the experimental line shape. Furthermore, comparing the simulation with the experiment, we find that the Breit interaction plays a very important role in the creation of the line profile observed in the experiment. We will detail our experiment procedure and present the results followed by a brief discussion.

The principle of the present experimental method is similar to that used by Ali *et al.* [7] and described in detail in our previous paper [6]. The experiment was performed for highly

charged Bi at the Tokyo EBIT [8]. Bi was continuously introduced into the EBIT using an effusion cell [9]. In the trap region of the EBIT, highly charged ions are produced through successive ionization by the energetic electron-beam impact. At equilibrium, the charge abundance of trapped ions is determined by the rates for ionization and recombination processes. Thus, the ion abundance ratio between Be-like and B-like Bi ions can be expressed in terms of cross sections of the relevant collision processes,

$$\frac{n_B}{n_{Be}} = \frac{\sigma_{Be}^{DR} + \sigma_{Be}^{RR} + \langle \sigma_{Be}^{CX} \rangle}{\sigma_B^{ion}}, \quad (2)$$

where σ_{Be}^{DR} and σ_{Be}^{RR} are the dielectronic and radiative recombination cross sections for Be-like Bi, σ_B^{ion} is the electron-impact ionization cross section for B-like Bi, and $\langle \sigma_{Be}^{CX} \rangle$ is the effective charge-exchange cross section [10] for collisions with the residual gas.

If there is no resonant state, i.e., $\sigma_{Be}^{DR}=0$, the ratio n_B/n_{Be} varies smoothly with the electron energy. However, when the electron incident energy (within the beam energy width) is close to the DR resonant energy, the abundance ratio in the trap changes drastically by an amount $\sigma_{Be}^{DR}/\sigma_B^{ion}$. Thus, the enhancement in the abundance ratio is proportional to the DR cross section of Be-like Bi over a narrow electron energy range, in which σ_B^{ion} can be regarded as a constant.

In this study, the abundance ratio was obtained by measuring the intensity of ions extracted from the EBIT. Ions escaping from the trap were extracted into a beam line [11]. After charge separation with an analyzing magnet, the extracted Be-like and B-like Bi were detected simultaneously with a position sensitive detector placed just after the magnet. It was assumed that the total efficiency (escape, transport, and detection) was the same for the adjacent charge state ions. This assumption was confirmed experimentally by comparing the charge state abundance obtained from the x-ray observation of trapped ions with that obtained from the extracted-ion observation [6]. The electron energy was stepwise scanned and counting of the ions was started 2 s after the electron energy was changed to ensure the charge equilibrium condition had been established and continued for 8 s.

The electron energy was calibrated through x-ray observation performed separately from the ion abundance measurements. In the calibration experiments, emitted x rays were observed with a Ge detector by injecting Kr from an ordinary gas injector at the same time as Bi was injected from the effusion cell. The electron energy was thus calibrated by observing RR x rays to $n=1$ levels of bare and H-like Kr ions similarly to the technique used in Ref. [12]. The error in the electron energy scale is considered to be about 30 eV, arising from the error in the x-ray energy calibration.

Figure 1 shows the result of a survey scan performed to obtain the electron energy dependence of the ratio between B-like and Be-like Bi in the *KLL* DR resonance region. As seen in the figure, enhancements due to DR of Be-like Bi are found around 51, 53.5, and 56 keV, which correspond to $KL_{12}L_{12}$, $KL_{12}L_3$, and KL_3L_3 , respectively (L_{12} denotes the $2s_{1/2}$ and $2p_{1/2}$ levels and L_3 denotes the $2p_{3/2}$ level). As

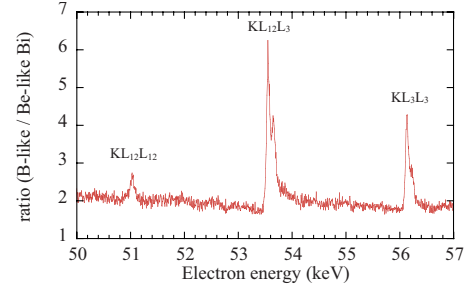


FIG. 1. (Color online) Abundance ratio between B-like and Be-like Bi at equilibrium in the EBIT with an electron-beam current of 80 mA. The enhancements around 51, 53.5, and 56 keV correspond to the *KLL* DR resonances of Be-like Bi.

shown in the figure, the $KL_{12}L_3$ resonances show a clear Fano profile, which can be confirmed by the fact that the peaks have an asymmetric shape and also that the background level is different on the lower- and higher-energy sides of the resonance.

In order to investigate the line shape in detail, the $KL_{12}L_3$ resonance was measured with a longer accumulation time to obtain higher statistical quality and a lower electron-beam current (50 mA) to get a better electron energy resolution. Figure 2(b) shows the result, for which acquisition took 12 h. Since the ionization cross section of the B-like ion is considered to be almost flat across this narrow energy range, the structures in Fig. 2(b) correspond to the relative DR cross sections for Be-like Bi. The right axis of Fig. 2(b) is the cross-section scale calibrated using the theoretical ionization cross section of B-like Bi (9.4×10^{-23} cm²).

Our previous x-ray observation [5] is also plotted in Fig. 2(a) for comparison. The x-ray measurement has the merit that the resonant state can be quasiresolved by selecting the integration area for x-ray energy. For example, by selecting one of the two final states ($J=1/2$ and $3/2$) for RR x rays, two peaks observed in the ion abundance measurement [Fig. 2(b)] can be separated as shown in Fig. 2(a). By narrowing the integration area further, the contribution from other charge states can be made smaller [4] as shown by the line “slice” in Fig. 2(a). However, the separation of the charge state is not perfect due to the limited x-ray energy resolution of a Ge detector. Hence, with x-ray observation it is difficult to assign the charge state, especially for small peaks, such as the one observed at around 53.6 keV in the $J=1/2$ cut. On the other hand, the ion abundance measurement can be compared straightforwardly with theory because the contribution from different charge states can be completely removed. In addition, the ion abundance measurement can give the integrated cross section; whereas the x-ray measurement gives a differential cross section for which the magnetic sublevel distribution should be taken into account. Thus, the present measurement provides another benchmark to test relativistic theories involving this interference.

To investigate the physical origin of the observed asymmetric resonant line profiles, we developed a theoretical method to calculate the recombination cross sections directly. The complete scattering state can be expressed as

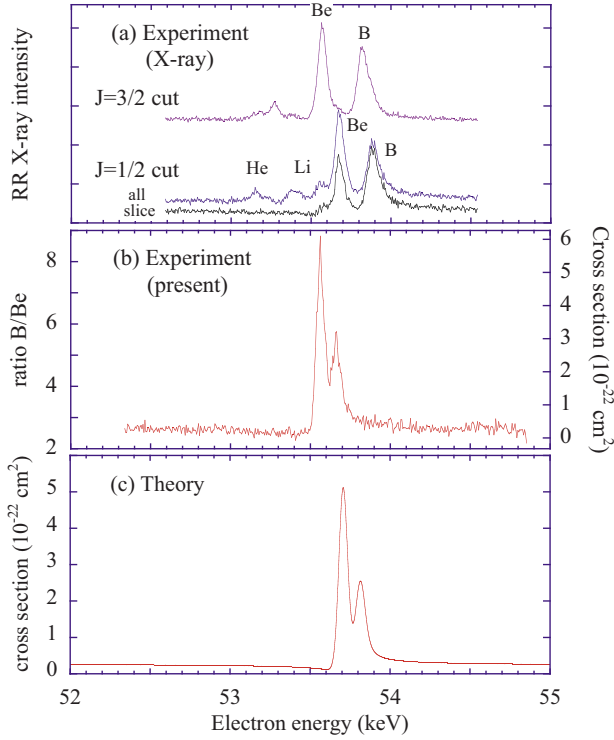


FIG. 2. (Color online) (a) Electron energy dependence of the x-ray intensity due to radiative recombination into the $J=3/2$ vacancies (“ $J=3/2$ cut”) and the $J=1/2$ vacancies (“ $J=1/2$ cut”). The result obtained with a narrower integrated x-ray energy width is indicated as “slice” (see text and Ref. [5] for the detail). (b) Abundance ratio between B-like and Be-like Bi ions at the equilibrium for the $KL_{12}L_3$ DR region (similar to Fig. 1 but the data in this figure were independently obtained with a longer accumulation time and a lower electron-beam current). (c) Theoretical result for the recombination cross section involving the resonant states. The data are convoluted with the experimental width (60 eV).

$$\begin{aligned}\Psi_c^+ &= G^+(E)[V_{res}(N) - V_{res}(N-1)]\Psi_0 + \Psi_0 \\ &= G^+(E)\tilde{V}_{res}\Psi_0 + \Psi_0,\end{aligned}\quad (3)$$

with $\Psi_0 = \Psi_g(N-1)\phi_c(\mathbf{r}_N)$, the initial state which is the product of the ground-state wave function for the $(N-1)$ -electron system and the incident electron wave function $\phi_c(\mathbf{r})$. $V_{res}(N)$, the difference between the total N -electron Hamiltonian and the N -independent-particle approximated single-electron Hamiltonians, is the residual interaction for the N -electron system. The independent-particle Hamiltonian is obtained from the relativistic density-functional theory with the self-interaction correction [13]. The configuration wave functions are constructed using the single-electron wave functions obtained from the single-electron Hamiltonian. The Green’s function $G^+(E)$ is calculated in the inner region with the time-propagation technique similar to the one used in antiproton atom collisions [14,15] with only one electron in continuum. The coupling coefficients of the spin-angular momentum and the multipole transition matrix used later on are calculated by the ANCO package of Gaigalas and Fritzsche [16]. The detailed theoretical procedure will be published elsewhere [17]. With the complete scattering wave function

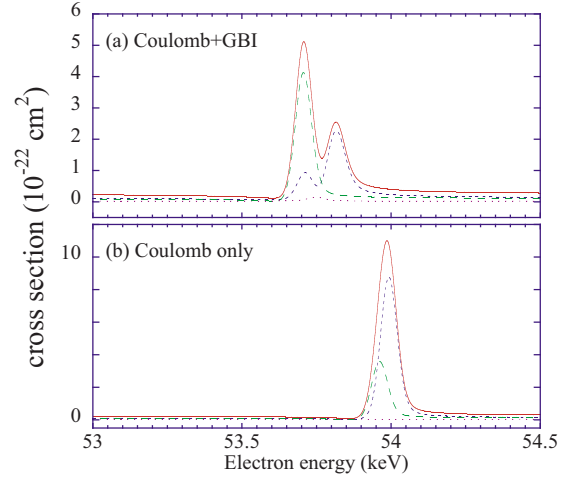


FIG. 3. (Color online) The total recombination cross section for Be-like Bi (solid line) and its partial contributions (long-dashed curve for the intermediate states with $J=5/2$; dashed curve for $J=3/2$ and dotted curve for $J=1/2$). (a) Results with the generalized Breit interaction [the solid line is the same as Fig. 2(c)]; (b) results considering only the Coulomb interaction. All results are convoluted with the experimental width (60 eV).

Ψ_c^+ , we calculated the radiative recombination cross sections involving the DR resonant states as shown in Fig. 2(c). As seen in Fig. 2, the peak position of the theoretical result differs from that of the experiment by about 150 eV, which is larger than the error in the experimental energy scale (about 30 eV). This difference may come from the contribution of the self-energy which is on the same order [18] and not included in the present calculation. Other than the peak position, however, the theory reproduced the experimental asymmetric line profile very well. Although two clear peaks are found in both the theory and the experiment, according to the calculated partial cross sections shown in Fig. 3(a), the lower-energy peak is considered to be composed of the contributions from the DR states with $J=5/2$ and $3/2$; whereas the higher-energy peak is considered to arise from the DR state with $J=3/2$ predominantly. The contributions from the DR state with $J=1/2$ are small for both the peaks.

The DR process is the inverse process of the photoabsorption followed by an Auger decay. The resonant state created by photoabsorption may also decay through radiative process (radiative damping), which is not directly related to the DR process. But the radiative damping affects the lifetime and the line profile of the DR state. We took into account this radiative damping effect in the present theoretical method.

It is also important to consider the contribution from the Breit interaction [19] since we are dealing with a very high- Z ion. Figure 3 shows theoretical cross sections calculated in two different ways; the calculation shown in Fig. 3(b) was obtained by considering only the Coulomb interaction, whereas that of Fig. 3(a) was obtained by taking the generalized Breit interaction. As seen in the figure, the Breit interaction affects the relative position of the resonances very strongly. The result with only the Coulomb interaction [Fig. 3(b)] completely failed to reproduce the experiment, whereas the calculations which included the Breit interaction [Fig.

3(a)] agree with the experiment shown in Fig. 2(b) very well. Thus, we can conclude that the Breit interaction also plays a crucial role in producing the line profile.

In conclusion, we have clearly demonstrated how the ion abundance measurement with extracted ions from an EBIT is effective to study the collision processes of electrons with highly charged heavy ions. Fano profiles arising from the interference between dielectronic recombination and radiative recombination have been observed for Be-like Bi with sufficiently high statistical quality to show that the Breit in-

teraction plays an important role for the asymmetrical line profile in comparison with our theoretical studies.

This work was supported by KAKENHI under Grant No. 21340111 and partially supported by the National Natural Science Foundation of China under Grants No.10674020 and No. 10434050. This work was also a part of the 21st Century Center of Excellence Program at UEC. F.J.C. and A.P.K. thank the Royal Society for support which allowed them to participate in this research program.

-
- [1] R. P. Madden and K. Codling, *Phys. Rev. Lett.* **10**, 516 (1963).
 [2] U. Fano, *Phys. Rev.* **124**, 1866 (1961).
 [3] D. A. Knapp, P. Beiersdorfer, M. H. Chen, J. H. Scofield, and D. Schneider, *Phys. Rev. Lett.* **74**, 54 (1995).
 [4] A. J. González Martínez, J. R. Crespo López-Urrutia, J. Braun, G. Brenner, H. Bruhns, A. Lapierre, V. Mironov, R. Soria Orts, H. Tawara, M. Trinczek, J. Ullrich, and J. H. Scofield, *Phys. Rev. Lett.* **94**, 203201 (2005).
 [5] H. Tobiya *et al.*, *J. Phys.: Conf. Ser.* **58**, 239 (2007).
 [6] H. Watanabe, H. Tobiya, A. P. Kavanagh, Y. M. Li, N. Nakamura, H. A. Sakaue, F. J. Currell, and S. Ohtani, *Phys. Rev. A* **75**, 012702 (2007).
 [7] R. Ali, C. P. Bhalla, C. L. Cocke, M. Schulz, and M. Stockli, *Phys. Rev. A* **44**, 223 (1991).
 [8] N. Nakamura *et al.*, *Phys. Scr.* **T73**, 362 (1997).
 [9] C. Yamada, K. Nagata, N. Nakamura, S. Ohtani, S. Takahashi, T. Tobiya, M. Tona, M. Sakurai, A. P. Kavanagh, and F. J. Currell, *Rev. Sci. Instrum.* **77**, 066110 (2006).
 [10] R. E. Marrs, S. R. Elliott, and D. A. Knapp, *Phys. Rev. Lett.* **72**, 4082 (1994).
 [11] N. Nakamura, H. Tobiya, H. Nohara, D. Kato, H. Watanabe, F. J. Currell, and S. Ohtani, *Phys. Rev. A* **73**, 020705(R) (2006).
 [12] N. Nakamura, T. Nakahara, and S. Ohtani, *J. Phys. Soc. Jpn.* **72**, 1650 (2003).
 [13] X. M. Tong and Shih-I Chu, *Phys. Rev. A* **57**, 855 (1998).
 [14] X. M. Tong, K. Hino, and N. Toshima, *Phys. Rev. Lett.* **97**, 243202 (2006).
 [15] X. M. Tong, K. Hino, and N. Toshima, *Phys. Rev. Lett.* **101**, 163201 (2008).
 [16] G. Gaigalas and S. Fritzsche, *Comput. Phys. Commun.* **148**, 349 (2002).
 [17] X. M. Tong, N. Nakamura, T. Watanabe, S. Ohtani, and N. Toshima (unpublished).
 [18] Z. Harman, I. I. Tupitsyn, A. N. Artemyev, U. D. Jentschura, C. H. Keitel, J. R. Crespo López-Urrutia, A. J. González Martínez, H. Tawara, and J. Ullrich, *Phys. Rev. A* **73**, 052711 (2006).
 [19] N. Nakamura, A. P. Kavanagh, H. Watanabe, H. A. Sakaue, Y. Li, D. Kato, F. J. Currell, and S. Ohtani, *Phys. Rev. Lett.* **100**, 073203 (2008).